CHEMPHYSCHEM

DOI: 10.1002/cphc.200800510

Bonding in Mercury Molecules Described by the Normalized Elimination of the Small Component and Coupled Cluster Theory

Dieter Cremer,*[a, b] Elfi Kraka,[a] and Michael Filatov[c]

Bond dissociation energies (BDEs) of neutral HgX and cationic HgX^+ molecules range from less than a kcal mol^{-1} to as much as 60 kcal mol^{-1}. Using NESC/CCSD(T) [normalized elimination of the small component and coupled-cluster theory with all single and double excitations and a perturbative treatment of the triple excitations] in combination with triple-zeta basis sets, bonding in 28 mercury molecules HgX (X = H, Li, Na, K, Rb, CH_3, SiH_3, GeH_3, SnH_3, NH_2, PH_2, AsH_2, SbH_2, OH, SH, SeH, TeH, O, S, Se, Te, F, Cl, Br, I, CN, CF_3, OCF_3) and their corresponding 28 cations is investigated. Mercury undergoes weak covalent bonding with its partner X in most cases (exceptions: X = alkali atoms, which lead to van der Waals bonding) although the BDEs are mostly smaller than 12 kcal mol^{-1}. Bonding is weakened by 1) a singly occupied destabilized σ-HOMO and 2) lone pair repulsion. The magnitude of σ*-destabilization can be determined from the energy difference BDE(HgX)−BDE(HgX^+), which is largest for bonding partners from groups IVb and Vb of the periodic table (up to 80 kcal mol^{-1}). BDEs can be enlarged by charge transfer from Hg and increased HgX ionic bonding, provided the bonding partner of Hg is sufficiently electronegative. The fine-tuning of covalent and ionic bonding, σ-destabilization, and lone-pair repulsion occurs via relativistic effects where 6s AO contraction and 5d AO expansion are decisive. Lone pair repulsion involving the mercury 5d AOs plays an important role in the case of some mercury chalcogenides HgE (E = O, Te) where it leads to $^3\Pi$ rather than $^1\Sigma^+$ ground states. However, both HgE($^3\Pi$) and HgE($^1\Sigma^+$) should not be experimentally detectable under normal conditions, which is in contrast to experimental predictions suggesting BDE values for HgE between 30 and 53 kcal mol^{-1}. The results of this work are discussed with regard to their relevance for mercury bonding in general, the chemistry of mercury, and reactions of elemental Hg in the atmosphere.*

1. Introduction

Mercury exists in elemental form in the atmosphere as a result of both natural and anthropogenic activities.[1–3] Estimates of global emissions of mercury to the atmosphere range from 2000 to 6000 tons per year.[4] The large uncertainties result from vague estimates of natural emission rates. Mercury can cycle between the atmosphere, land, and water and during this process it undergoes a series of complex biological, chemical, and physical transformations, many of which are not completely understood.[5,6] Humans, plants, and animals are exposed to mercury and accumulate it during this cycle, potentially resulting in a variety of ecological and human health impacts.[7,8] Recent studies in both the Arctic and Antarctic have revealed that elemental gaseous mercury is depleted from the atmosphere at certain times of the year and deposited in the snow-pack, which brings it into the biosphere.[9–14] Mercury depletion events seem to correlate with tropospheric ozone reduction,[9–11,13,14] which is known to be a result of the catalytic destruction of ozone molecules by chlorine and bromine atoms, thus yielding molecular oxygen and ClO or BrO.[15–17] In this connection, the reaction Hg + BrO → HgO + Br has been proposed as an important path for mercury depletion in the troposphere.[10,13,16]

Various authors have pointed out that the experimentally derived stability of gaseous HgO is seriously in error[18,19] and that by correcting for this error there is no chance that elemental Hg can be oxidized by BrO or other related oxidants in the atmosphere. Filatov and Cremer[19] have shown that observations made with regard to the stability of HgO and its bond dissociation energy (BDE) may also apply to stability and bonding of other mercury chalcogenides HgE. There is a distinctive dichotomy when it comes to a description of mercury bonding. Huber and Herzberg[20] list a number of weakly bound HgX compounds with BDEs smaller than 10 kcal mol^{-1} that suggest that mercury might prefer van der Waals complex formation. However in the case of the mercury chalcogenides and halides, experimental BDEs suggest relatively strong covalent bonding (BDE values up to 50 kcal mol^{-1}).[20] A pronounced increase in the HgX bond strength is also found when considering the cations of HgX molecules, which turn out to have bond strengths up to 60 kcal mol^{-1} as we show herein.

[a] Prof. Dr. D. Cremer, Prof. Dr. E. Kraka
Department of Chemistry
University of the Pacific, 3601 Pacific Avenue
Stockton, CA 95211 (USA)
E-mail: dcremer@pacific.edu

[b] Prof. Dr. D. Cremer
Department of Physics
University of the Pacific, 3601 Pacific Avenue
Stockton, CA 95211 (USA)

[c] Prof. Dr. M. Filatov
Zernike Institute for Advanced Materials
University of Groningen, Nijenborgh 4
9747 AG Groningen (The Netherlands)

An understanding of mercury bonding is essential to anticipate possible reactions of elemental Hg in the polluted atmosphere. There have been several quantum chemical studies of mercury compounds,[18,19,21–44] where those of the Peterson group[18,21–28] and those by Tossell[29–33] are most noteworthy. Each of these investigations focused on selected mercury compounds HgX; however none of them attempted a comprehensive study of mercury bonding by varying X systematically within the periodic table. Due to this, we have decided to investigate the reaction of gaseous mercury with 28 different bonding partners X from five different main groups and four different periods of the periodic table—thus thoroughly testing the possible bonding situations that may occur between Hg and other atoms or small radicals. The investigation is based on high-level relativistic ab initio theory with infinite-order electron correlation effects. It is aimed at answering the following questions:

1) How does mercury bonding vary in dependence of its partner and which atoms or functional groups form the most stable mercury bonds?
2) Can one explain variations in mercury bonding using simple models of the chemical bond successfully applied to bonding between less heavy atoms?
3) How do relativistic effects influence mercury bonding?
4) Can relativistic ab initio theory satisfactorily describe the stability and bond strengths of compounds HgX?
5) Is the discrepancy between theory and experiment found for HgO, HgS, and HgSe an exception or does it also occur for other HgX molecules?
6) Which chemical reactions can add to the depletion of elemental Hg from the atmosphere?

Computational Methods

Mercury is known to have strong scalar relativistic effects.[18,19,21–44] Therefore, we have used two levels of relativistic theory. Preliminary calculations were carried out employing the zeroth order regular approximation with gauge independence (ZORA–GI) method[45] and density functional theory (DFT) with the B3LYP hybrid functional[46–48] to obtain suitable starting geometries. Then, the quantum chemical description was improved by employing 1) the normalized elimination of the small component (NESC)[49] that presents a more complete method for determining scalar relativistic effects and b) coupled-cluster theory including all single (S) and double (D) excitations and a perturbative treatment of the triple excitations (T), thus yielding CCSD(T).[50] In addition, all atoms and molecules were calculated at the non-relativistic B3LYP and CCSD(T) levels of theory to obtain reference values for determining the relativistic corrections needed in connection with the discussion of HgX bonding. Since relativistic effects on molecular geometries have been amply discussed, we only report the energy correction obtained by calculating non-relativistic BDEs at relativistic geometries. Hence, five different levels of description were applied: 1) B3LYP, 2) CCSD(T), 3) ZORA–GI/B3LYP, 4) NESC/B3LYP, 5) NESC/CCSD(T). Geometry optimizations were repeated at level 4 to verify the level 3 results, which, in most cases, differed only slightly. At level 5, only single-point calculations were carried out apart from those cases where experimental bond lengths were available.

For Hg, we used a (22s19p12d9f) basis set of Dyall[51] that was converted via the contraction scheme (222231211111111/5311111111111/42111111/42111) to a [15s13p8d5f] contracted basis. The contraction was carried out to minimize basis set superposition errors (BSSE), which was tested by assessing BSSE via the counterpoise method.[52] In all cases tested, the BSSE was reduced to less than 0.5 kcal mol^{-1} and was not considered any longer. The Hg basis set is of double-zeta quality for the core orbitals, but of triple-zeta quality in the valence space. Therefore it was combined with the aug-cc-pVTZ basis sets of Dunning for elements of the first three periods.[53] For K, a 6-311++G(3df) basis was employed[54] whereas for 4th period elements the following Dyall basis sets were used: Rb: (21s15p9d1f)[14s10p5d1f], Sn: (21s15p11d1f)[14s10p7d1f], Sb: (21s15p11d1f)[13s10p7d1f], Te: (22s16p12d2f)[12s11p7d2f] and I (22s16p12d2f)[12s11p7d2f].[51]

The electron density distribution was calculated at NESC/B3LYP and then the natural bond order (NBO) analysis was applied to determine orbital population values and atomic charges.[55] In addition, the electron density $\rho(\mathbf{r}_c)$ and the energy density $H(\mathbf{r}_c)$ at the bond critical point $\mathbf{r}_c$ were computed to identify the character of the bonding interactions according to the Cremer–Kraka criteria.[56] Dipole moments were calculated for the cations with regard to the center of charge to make a comparison meaningful.

For the analysis of the calculated BDE values, we calculated orbital energies of Hg and X to investigate how the energies of the frontier orbitals for different substituents X compare to those of Hg. For this purpose, Hg and X were positioned at a distance of 10 Å to impose the symmetry of the diatomic molecule HgX, but to suppress interactions. Calculations were carried out with NESC/HF where the unrestricted methodology was applied. In special cases (alkali atoms), the energy of the HOMO can be compared with the experimental ionization potential (IP). However, in most other cases the orbital energies needed for the bonding analysis are not reflected by measured IPs as is discussed in section 2.

All calculations were carried out with the program packages COLOGNE08[57] and Gaussian 03.[58]

2. Results and Discussions

In Tables 1 and 4, all calculated BDE values for molecules HgX are summarized together with the corresponding bond lengths, dipole moments, ionization potentials (IPs), and NBO charge transfer values. On average, CCSD(T) energies differ from B3LYP values by 2–3 kcal mol^{-1}. Since the former are more reliable, only the NESC/CCSD(T) BDEs are discussed.

2.1. Possible Models for Describing Mercury Bonding

Mercury possesses a [Xe]4f^{14}5d^{10}6s^2 electron configuration, which makes it valence isoelectronic with Be, Mg, and so forth. Hence, bonding might only be established if one of the 6s electrons is promoted to a 6p orbital (hybridization model). Alternatively, a donor–acceptor complex can be formed, accompanied by significant charge transfer from mercury to a suitable acceptor (charge transfer model). A more general description of bonding involving mercury may be based on the details of three-electron bonding that depends on AO overlap

Table 1. Calculated properties of HgX molecules. The bond lengths *R*(HgX) are calculated at the NESC/B3LYP level of theory and in some cases at the NESC/CCSD(T) level of theory (numbers in parentheses). Non-relativistic B3LYP and CCSD(T) calculations of HgX molecules are at NESC/B3LYP geometries. The charge values *q*(Hg) are based on NESC/B3LYP calculations with the NBO method and give the transfer of charge from Hg to X. Positive dipole moments are oriented from Hg to X (chemical notation).

Molecule	BDE B3LYP [kcal mol^{-1}]	BDE NESC/B3LYP [kcal mol^{-1}]	R(HgX) [Å]	Charge q(Hg) [electron]	Dipole moment μ [Debye]	BDE CCSD(T) [kcal mol^{-1}]	BDE NESC/CCSD(T) [kcal mol^{-1}]	IP NESC/B3LYP [kcal mol^{-1}]	IP NESC/CCSD(T) [kcal mol^{-1}]
HgH ($^2\Sigma^+$)	21.2	11.7	1.784 (1.749)	0.332	0.38	20.8	10.0	188.4	183.3
HgLi ($^2\Sigma^+$)	5.3	4.4	2.917 (3.056)	−0.022	0.28	4.1	2.9	119.2	112.3
HgNa ($^2\Sigma^+$)	3.6	3.0	3.333 (3.432)	−0.020	0.47	2.8	2.3	118.1	111.7
HgK ($^2\Sigma^+$)	2.5	2.0	3.830 (4.197)	−0.031	0.58	0.6	0.8	100.8	94.2
HgRb ($^2\Sigma^+$)	2.2	0.7	4.052 (4.417)	−0.030	0.64	0.2	0.7	97.5	91.0
$HgCH_3$ ($^2A_1$)	10.4	1.7	2.455	0.234	0.23	12.6	3.0	172.1	167.9
$HgSiH_3$ ($^2A_1$)	13.1	5.7	2.735	0.206	0.12	15.2	6.3	159.2	155.8
$HgGeH_3$ ($^2A_1$)	13.4	5.4	2.824	0.226	0.21	14.2	5.4	159.0	155.1
$HgSnH_3$ ($^2A_1$)	11.5	5.8	3.054	0.199	0.36	10.1	3.0	155.9	150.9
HgCN ($^2\Sigma^+$)	52.4	31.6	2.159	0.621	4.61	55.5	32.6	218.3	213.6
$HgCF_3$ ($^2A_1$)	9.6	1.9	2.617	0.164	1.47	10.1	2.7	192.4	189.2
$HgNH_2$ ($^2A'$)	17.1	4.4	2.383	0.299	1.21	18.7	4.2	195.3	188.3
$HgPH_2$ ($^2A'$)	11.5	3.4	2.843	0.183	0.58	12.7	3.6	177.2	174.0
$HgAsH_2$ ($^2A'$)	10.3	4.0	3.010	0.156	0.38	10.6	4.5	174.5	171.9
$HgSbH_2$ ($^2A'$)	8.0	4.0	3.216	0.119	0.47	6.0	1.9	167.4	164.1
HgOH ($^2A'$)	34.1	13.3	2.181	0.494	1.92	37.5	12.4	214.7	206.6
HgSH ($^2A'$)	25.9	9.9	2.579	0.371	1.70	28.4	9.8	198.2	193.7
HgSeH($^2A'$)	22.7	7.9	2.776	0.301	1.50	23.9	7.5	194.2	190.2
HgTeH ($^2A'$)	18.2	6.8	2.948	0.252	1.18	18.0	5.9	185.8	181.4
$HgOCF_3$ ($^2A'$)	47.2	18.8	2.203	0.635	4.39	48.4	22.2	231.0	223.6
HgO ($^3\Pi$)	26.8	9.7	2.231	0.428	2.05	26.8	3.5	225.7	219.1
HgS ($^3\Pi$)	23.0	8.4	2.600	0.341	1.64	21.8	5.7	202.8	199.6
HgSe ($^3\Pi$)	19.7	6.0	2.835	0.264	1.43	17.7	3.7	198.7	196.4
HgTe ($^3\Pi$)	16.2	5.8	2.970	0.223	1.09	12.0	2.6	188.4	184.9
HgF ($^2\Sigma^+$)	62.6	33.6	2.080	0.672	3.30	64.2	30.9	235.3	226.7
HgCl ($^2\Sigma^+$)	46.8	22.6	2.460	0.542	2.99	49.0	21.4	219.5	213.5
HgBr ($^2\Sigma^+$)	39.8	16.1	2.672	0.474	2.87	41.1	14.4	214.7	209.0
HgI ($^2\Sigma^+$)	31.3	13.6	2.820	0.383	2.34	30.5	10.9	204.3	197.9

and the energy difference between the orbitals involved in bonding (three-electron two-orbital model). For weak bonding interactions, one might just consider the polarizability of mercury and that of its bonding partner and describe the less stable mercury compounds as van der Waals complexes (van der Waals bonding model). All these bonding models may have some relevance for describing mercury bonding. However, in addition to these bonding models, one has to consider the influence of relativistic effects that may change the bonding substantially.

Whenever using orbital models for heavy atoms one has to consider spin–orbit coupling (SOC). Strong SOC can lead to a mixing of σ- and π-orbitals and thereby conclusions drawn from a nonrelativistic MO model are no longer valid. In the case of mercury, SOC is normally small. For example, Peterson and co-workers[59] recently investigated SOC for the mercury chalcogenides using multireference configuration interaction theory. They found that changes in the BDEs caused by SOC were between 0.5 (HgS) and 1.7 kcal mol^{-1} (HgO). These values, although they do not provide proof, suggest that orbital mixing should be small and that a non-relativistic MO model can explain HgX bonding on a qualitative basis.

2.1.1. Hybridization Model

For all HgX molecules considered herein, we calculated the NBO orbital populations. The population of the 6p(Hg) AOs never exceeds 0.1 electron and is mostly much smaller. Obviously, hybridization does not play any role, due to the high energy of the mercury 6p AOs. The first two excited states of Hg involving the 6p orbitals (^{3}P and ^{1}P) are 120 and 153 kcal mol^{-1} above the ground state,[61] which confirms that

only strong electron donors can lead to the population of the 6p AOs. Nevertheless, the correct description of the ^{1}P state of Hg is important to account for the dispersion interactions in van der Waals molecules correctly. Also relevant in this connection is the fact that there is no significant 5d or 4f participation in bonding because their populations are always close to 10 and 14 electrons, respectively (deviations of <0.07 electrons for the d AOs and <0.02 electrons for the f AOs occur). This seems to be different from the solid state where the 5d electrons make a significant contribution to bonding in solid HgO.[61] However for the gas phase, one can exclude hybridization involving significant participation of either 6p, 5d, or 4f AOs in connection with mercury bonding.

2.1.2. Charge Transfer Model

Figure 1 gives the NESC/CCSD(T) BDE values for the mercury halides as a function of the charge transfer from Hg to the halogen atom X (X = F to I). There is a clear increase of BDE(HgX)

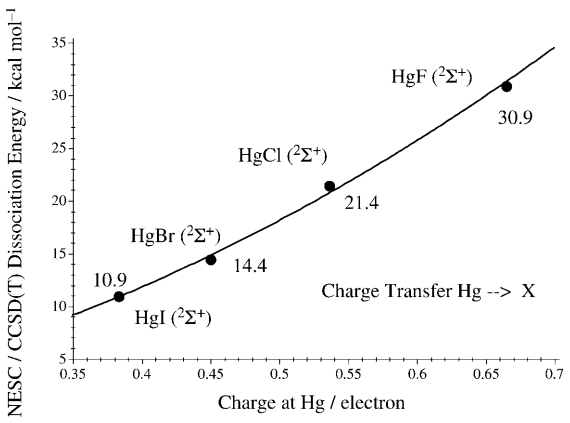

Figure 1. HgX (X = F, Cl, Br, I) BDE values as a function of the charge transfer from Hg to X calculated at the NESC/CCSD(T) level of theory.

from 11 to 31 kcal mol^{-1} depending on the charge transfer from Hg to the X atom, which in turn depends on the electronegativity of the halogen. For X = F, the largest charge transfer (0.672 electron) and the largest BDE value (30.9 kcal mol^{-1}, Table 1) is obtained.

This trend is even more pronounced for the non-relativistic BDE values (X = F: 0.866 electron), which are significantly larger than the relativistic ones. The large difference (20–34 kcal mol^{-1}) between the CCSD(T) [30–64 kcal mol^{-1}, Table 1] and NESC/CCSD(T) BDE values (10–30 kcal mol^{-1}) in the case of the Hg halides indicates strong scalar relativistic effects resulting predominantly from the contraction of the 6s(Hg) orbital. Contraction leads to lowering of the 6s orbital energy, which in turn makes the 6s electrons less accessible to charge transfer and thereby causes a drastic decrease of the relativistic BDE values compared to the non-relativistic ones (Table 1).

Inspection of all relativistically corrected coupled-cluster BDEs calculated for some 28 mercury compounds (Table 1) reveals that their values, apart from a few exceptions, are rather small and more typical of van der Waals complexes than of covalently bonded mercury compounds. There is no gradual reduction of the bond strength in dependence of decreasing electronegativity as one might expect when proceeding from right to left within a period. Obviously, charge transfer depending on the electronegativity difference between Hg and X cannot be the only factor determining the strength of the HgX bond.

2.1.3. Three-Electron Two-Orbital Model of Mercury Bonding

In general, the bond strength is determined by a covalent part depending on the overlap between the interacting AOs, and an ionic part depending on the electronegativity difference between the bonding partners and the resulting charge transfer. There is a continuous change from covalent to ionic bonding, so that it is difficult to define an unambiguous borderline between the two kinds of bonding. Covalent bonding is mostly complemented by some ionic bonding and vice versa. Nevertheless, we simplify the discussion herein by speaking of (dominant) covalent or ionic bonding without explicitly referring to the complementing part of bonding. Ionic bonding strongly contributes to the strength of the HgX bond in some cases, as pointed out in section 2.1.2. However, it has to be clarified to what degree covalent bonding can also influence the HgX bond.

According to molecular orbital (MO) theory, the mercury 6s AO can combine with a s- or pσ AO of a partner atom to form a bonding (σ) and an antibonding (σ*) MO where the former is less stabilized than the latter is destabilized ($\Delta E_a > |\Delta E_b|$, see Table 2). This implies that in a three-electron case and the occupation of the σ* MO by a single electron, the bond strength is less than half as large as in the two-electron case. The stabilization (destabilization) of the σ (σ*) MO is largest for comparable or equal energies ($\Delta\varepsilon = 0$) of the starting AOs, but becomes smaller for $\Delta\varepsilon \neq 0$. The larger the electronegativity difference between the Hg and its bonding partner, the larger $\Delta\varepsilon$ becomes and the smaller the covalent character of the bond is, whereas the ionic character increases. One can assess this situation by comparing the appropriate orbital energies of the bonding partners as done for some group IA, VIB, VIIB elements and Hg in Table 2.

The 6s orbital energy of Hg is −8.8 eV (Table 2; the first IP is 10.44 eV,[62] where the 1.6 eV increase in the orbital energy is partly due to charge repulsion at 10 Å), which is higher than any of the *n*pσ orbital energies of the halogens or chalcogens. The difference $\Delta\varepsilon$ decreases within a group so that iodine (tellurium) has stronger 6s-*n*pσ orbital interactions with Hg than any of its lower homologs (Table 2). Hence, HgI (HgTe) bonding should be more covalent than any of the lower homologs. Covalent bonding is, however strongly reduced because of the occupation of the σ* MO by a single electron. The weakening of the HgX bond for X = I can be assessed by utilizing the thermodynamic cycle shown in Scheme 1.

The IP of molecule HgX when compared with the first IP of mercury gives a measure of the destabilization of the σ* MO relative to the energy of the 6s(Hg) AO. According to the cycle

Table 2. σ-Type bonding and antibonding molecular orbitals of HgX that are formed from 6s(Hg) and pσ(X). In the upper graphic equal (or similar) energies of the starting AOs are assumed, that is, $\Delta\varepsilon \approx 0$, valid when X = SnH_3. In the lower graphic different starting energies are assumed for the AOs, that is, $\Delta\varepsilon > 0$ (X = F) or < 0 (X = Li). The (de)stabilization of the (anti)-bonding MO is indicated. Orbital energies from NESC/UHF calculations obtained for HgX at a Hg–X distance of 10 Å are also given for Hg and its bonding partners (6s and 5d for Hg, highest σ and π for X, [eV]).

Orbital Energies, $-\varepsilon$ [eV]; (Ionization Potential, IP [eV])

H	13.6 (1s)					Hg	8.8 (6s), 16.3 (5d)
	(13.6)						(10.44)
Li	5.3 (2s)	CH_3	11.0	O	19.3	F	23.0 pσ
	(5.4)				16.6		19.9 pπ
Na	5.0 (3s)	SiH_3	9.4	S	13.2	Cl	15.8 pσ
	(5.1)				11.3		13.7 pπ
K	4.0 (4s)	GeH_3	9.2	Se	12.2	Br	14.3 pσ
	(4.3)				10.5		12.4 pπ
Rb	3.8 (5s)	SnH_3	8.7	Te	19.8	I	12.5 pσ
	(4.2)				9.4		10.9 pπ

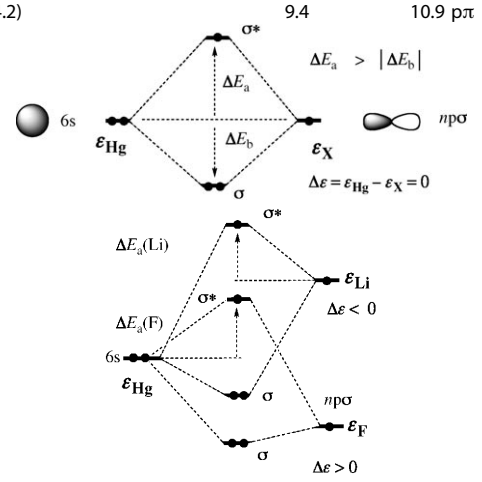

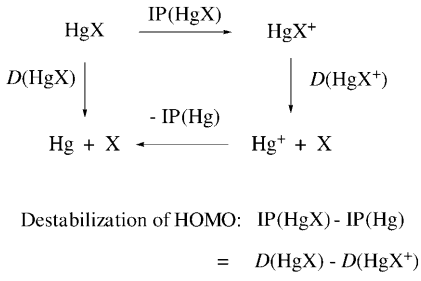

Destabilization of HOMO: IP(HgX) - IP(Hg)
= D(HgX) - D(HgX+)

Scheme 1. Thermodynamic cycle to determine the destabilization energy of the σ*(HgX) MO of Table 3. IP: Ionization potential, *D*: bond dissociation energy

shown in Scheme 1 this destabilization energy is exactly equal to the difference in the BDEs of neutral HgX and its cation. The destabilization of the σ* MO should be lowest when X is a strongly electronegative partner such as F that prefers predominantly ionic bonding, whereas it should be largest for a bonding partner such as I that binds more covalently than F.

Before discussing the destabilization energies ΔE_a of HgX molecules, it first has to be clarified whether HgX^+ always dissociates according to Scheme 1 into $Hg^+ + X$ (reaction I). For X = Li, Na, K, Rb, there should be a dissociation into $Hg + X^+$ (reaction II) according to the electropositive character and the low IPs of the alkali atoms. Accordingly, one has to take as a reference the calculated IP of the alkali rather than the Hg atom and to consider the correct dissociation reaction to get reasonable dissociation energies. However, one can relate the destabilization energies based on the different dissociation reactions I and II in the case of the alkali atoms by Equation (1):

$$\Delta E_a(\mathrm{I}) = \Delta E_a(\mathrm{II}) + \mathrm{IP(Hg)} - \mathrm{IP(alkali)} \quad (1)$$

There are other cases where the available IP of X suggests dissociation reaction II. However for all HgX^+ molcules investigated herein (Table 1), except when X is an alkali atom, the electronegativity of X is always larger than that of Hg, which is confirmed by the calculated charge distribution (Table 1). Hg donates negative charge to X. This shows that even for dissociation according to reaction II, it is appropriate to use destabilization energy ΔE_a(I) rather than ΔE_a(II). This is a result of the fact that the relevant orbital energy ε_X of an atom or functional group X in the valence state, hybridization state, or geometry of the bonding situation is lower (the IP is larger) than that of free X. Therefore, we follow the calculated charge transfer to determine destabilization energies [apart from X = alkali, always ΔE_a(I)], whereas both reactions I and II have been calculated to determine the stability of HgX^+ given by the lowest BDE value [either BDE(I) or BDE(II)].

The NESC/CCSD(T) BDEs of all HgX and HgX^+ molecules investigated herein are given in Table 3 together with the destabilization energies of the σ*(HgX) MO. We first consider molecules where X is not an alkali. For mercury halides, we calculate an inversion in the bond strengths in the case of the monocations as compared to the neutral systems. Although the HgI bond has the lowest ionic character (Figure 1), it has the highest covalent character, which implies a large stabilization of the σ MO and, consequently, a large destabilization of 36 kcal mol^{-1} of the σ* MO. Accordingly, HgI has a rather weak bond of just 10.9 kcal mol^{-1} whereas the BDE for HgI^+ is 47.2 kcal mol^{-1}.

As shown in Table 3, the HgX bond strength increases within a group and from right to left within a period up to group IVB for the monocations. However, the destabilization of the σ*(HgX) MO increases in the same way (up to 83 kcal mol^{-1}, X = SnH_3) so that the HgX bond strength decreases as a consequence. All HgX molecules, with the exception of the mercury halides, HgCN, and $HgOCF_3$, possess BDE values between 3 and 12 kcal mol^{-1}. However for the corresponding cations the bond strength is much larger (up to 70 kcal mol^{-1}, Table 4), thus reflecting the actual strength of two-electron bonding. These trends are also reflected by the HgX bond lengths (Table 1; up to 0.3 Å shorter for the cations than for the neutral molecules).

In the upper half of Table 3, the BDE values of the mercury cations dissociating according to reaction I: $HgX^+ \rightarrow Hg^+ + X$, are given, whereas BDE values of the alternative dissociation reaction II: $HgX^+ \rightarrow Hg + X^+$ are listed in the lower half. Table 4 lists the BDE values of the preferred dissociation process in bold. In those cases in which the electronegativity of X is

Table 3. NESC/CCSD(T) BDE values of 28 HgX molecules and their corresponding cations HgX^+ (in bold). The destabilization energy of the σ* MO, calculated according to the thermodynamic cycle of Scheme 1, is also given (in parentheses below X). All energies are given in kcal mol^{-1}. Top: dissociation of HgX^+ into $Hg^+ + X$. Bottom: dissociation of HgX^+ into $Hg + X^+$.

NESC/CCSD(T) bond dissociation energies for $HgX^+ \rightarrow Hg^+ + X$ [kcal mol^{-1}]

H	10.0										
(50.9)	**60.9**										
Li	2.9	CH_3	3.0	NH_2	4.2	OH	12.4	O	3.5	F	30.9
		(66.2)	**69.2**	(45.8)	**50.0**	(27.6)	**39.9**	(14.8)	**18.6**	(7.4)	**38.3**
Na	2.3	SiH_3	6.3	PH_2	3.6	SH	9.8	S	5.7	Cl	21.4
		(78.3)	**84.6**	(60.2)	**63.8**	(40.6)	**50.3**	(34.5)	**40.2**	(20.6)	**42.0**
K	0.8	GeH_3	5.4	AsH_2	4.5	SeH	7.5	Se	3.7	Br	14.4
		(79.1)	**84.5**	(62.2)	**66.7**	(44.0)	**51.5**	(37.9)	**41.6**	(25.1)	**39.5**
Rb	0.7	SnH_3	3.0	SbH_2	1.9	TeH	5.9	Te	2.6	I	10.9
		(83.3)	**86.3**	(70.0)	**71.9**	(52.8)	**58.7**	(49.2)	**51.8**	(36.3)	**47.2**
		CF_3	2.7			OCF_3	22.2				
		(44.6)	**47.3**			(10.5)	**32.7**				
		CN	32.6								
		(20.6)	**53.2**								

NESC/CCSD(T) bond dissociation energies for $HgX^+ \rightarrow Hg + X^+$ [kcal mol^{-1}]

Li	2.9	CH_3	3.0						
(10.9)	**13.8**	(57.7)	**60.7**						
Na	2.3	SiH_3	6.3	PH_2	3.6				
(3.9)	**6.2**	(29.9)	**36.2**	(51.4)	**55.0**				
K	0.8	GeH_3	5.4	AsH_2	4.5	SeH	7.5		
(4.2)	**5.0**	(27.9)	**33.3**	(43.0)	**48.5**	(30.8)	**38.3**		
Rb	0.7	SnH_3	3.0	SbH_2	1.9	TeH	5.9	Te	2.6
(3.7)	**4.4**	(21.4)	**24.4**	(32.4)	**34.3**	(17.1)	**23.0**	(34.3)	**36.9**
		CF_3	2.7						
		(19.0)	**21.7**						

smaller than that of Hg (alkali atoms), dissociation according to II is preferred and the thermodynamic cycle in Scheme 1 has to be modified in the way that IP(X) rather than IP(Hg) is used to determine the stabilization energy of the σ* MO (relative to the σ MO of X). However, there are HgX molecules for which, despite a larger electronegativity of X, dissociation II is still preferred (X = CH_3, SiH_3, etc., see Table 3 and Tables 1 and 4). The dissociation reaction first follows process I according to the electronegativity difference between Hg and X before a charge transfer from X to Hg leads to the path of dissociation II. The latter step is because X has a lower IP than Hg and, accordingly, the charge transfer yields a lower (preferred) BDE.

2.1.4. Lone Pair Repulsion

In Figure 2, perspective drawings of the four highest occupied MOs of HgF ($^2\Sigma^+$) are shown together with the corresponding MO diagram. Between the σ and σ* MOs, there is a degenerate set of occupied π* MOs, which is formed from the 5d(Hg) and 2p(X) AOs. Occupation of the π* MOs annihilates the stabilizing effect of the π-bonding electrons (see MO Scheme in Figure 2), and adds to the destabilization of the HgX bond. This effect is often described in a more general way as the lone pair repulsion effect. Its magnitude can be estimated by comparing the 5dπ and npπ orbital energies of Hg and X, respectively (Table 2). According to this comparison, π* destabilization (and thereby bond weakening due to lone pair repulsion) should be strongest for F and weakest for I. It should be even stronger for O (16.6 vs 16.3 eV, Table 2). This effect can be assessed more quantitatively with the help of the calculated relativistic BDE corrections as is discussed in the following.

2.2. Relativistic Effects on Hg Bonding

The major scalar relativistic effect results from a contraction of the 6s(Hg) AO. It has a number of consequences, of which already two have been mentioned: 1) Because of contraction, the 6s orbital energy decreases with the consequences for covalent bonding and σ* destabilization just described. 2) The decrease in the 6s AO energy makes charge transfer from Hg to X more difficult and thus reduces the ionic character and strength of the bond. There is however a third consequence of relativistic 6s AO contraction, which has to do with an increased shielding of the nucleus. The 5d electrons no longer feel the Hg nucleus that strongly and, accordingly, the 5d AOs expand and their orbital energies increase in value. This leads to a change in orbital repulsion (π* destabilization), which should be reflected by the relativistic corrections of the BDE values.

In Table 5, the nonrelativistic BDE values (NESC/B3LYP calculations) are compared with the relativistic corrections. For the cations (Table 5 b), the relativistic correction should be positive, thus increasing the BDE. It should be dominated by the con-

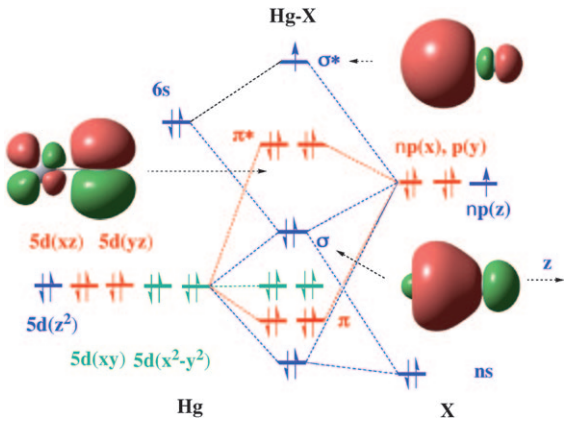

Figure 2. MO diagram for the nine highest occupied orbitals of a mercury halide $HgX(^2\Sigma^+)$. The σ-orbitals (blue), π-orbitals (red), and non-bonding orbitals (green) are indicated. For the highest MOs, computer drawings of the calculated orbitals are given.

Table 4. Calculated properties of HgX^+ molecules. BDEs of the cations HgX^+ are given with regard to dissociation reaction I: $HgX^+ \rightarrow Hg^+ + X$ (second entry), in some cases also with regard to dissociation II: $HgX^+ \rightarrow Hg + X^+$ (first entry). When two BDE values are given, the most likely BDE value that determines the stability of the cation is given in bold. In the case of the chalcogenides HgE^+, dissociation to $Hg^+(^2S) + E(^3P)$ (dissociation I) and $Hg(^1S) + E^+(^2D)$ (dissociation II) is considered. The bond lengths *R*(HgX) are calculated at the NESC/B3LYP level of theory and in some cases at the NESC/CCSD(T) level of theory (numbers in parentheses). Non-relativistic B3LYP and CCSD(T) calculations of HgX molecules are at NESC/B3LYP geometries. The charge values *q*(Hg) are based on NESC/B3LYP calculations with the NBO method and give the transfer of charge from Hg to X. Positive dipole moments are oriented from Hg to X (chemical notation).

Molecule	BDE B3LYP [kcal mol^{-1}]	BDE NESC/B3LYP [kcal mol^{-1}]	R(HgX) [Å]	Charge q(Hg) [electron]	Dipole moment μ [Debye]	BDE CCSD(T) [kcal mol^{-1}]	BDE NESC/CCSD(T) [kcal mol^{-1}]
HgH^+ ($^1\Sigma^+$)	41.0	63.2	1.606 (1.597)	0.959	0.30	39.6	60.9
$HgLi^+$ ($^1\Sigma^+$)	83.5; **17.7**	125.1; **14.9**	2.674 (2.709)	0.090	9.18	16.5	13.8
$HgNa^+$ ($^1\Sigma^+$)	83.5; **13.0**	124.8; **10.1**	3.031 (3.097)	0.070	10.36	15.7	6.2
HgK^+ ($^1\Sigma^+$)	97.8; **6.0**	141.0; **5.3**	3.521 (3.551)	0.029	11.54	5.3	5.0
$HgRb^+$ ($^1\Sigma^+$)	101.8; **4.6**	143.1; **3.3**	3.726 (3.735)	0.021	10.31	4.2	4.4
$HgCH_3^+$ ($^1A_1$)	45.7	69.5; **58.1**	2.168	0.872	1.97	45.8	69.2; **60.7**
$HgSiH_3^+$ ($^1A_1$)	53.2	86.4; **34.5**	2.574	0.561	3.25	51.7	84.6; **36.2**
$HgGeH_3^+$ ($^1A_1$)	54.0	86.2; **31.1**	2.664	0.545	1.48	51.6	84.5; **33.3**
$HgSnH_3^+$ ($^1A_1$)	54.3	89.8; **26.6**	2.865	0.525	0.55	50.6	86.3; **24.4**
$HgCN^+$ ($^1\Sigma^+$)	47.3	**53.2**; 162.9	2.000	1.272	3.94	49.4	**53.2**; 162.9
$HgCF_3^+$ ($^1A_1$)	24.4	49.3; **26.7**	2.354	0.633	0.26	25.0	47.3; **21.7**
$HgNH_2^+$ ($^1A'$)	36.8	**49.0**; 103.7	2.066	1.108	1.38	39.7	**50.0**; 102.2
$HgPH_2^+$ ($^1A'$)	42.1	66.1; **55.0**	2.480	0.732	2.14	41.6	63.8; **55.0**
$HgAsH_2^+$ ($^1A'$)	44.4	69.4; **48.1**	2.599	0.686	1.29	42.7	66.7; **48.5**
$HgSbH_2^+$ ($^1A'$)	45.9	76.5; **37.8**	2.807	0.558	1.17	42.6	71.9; **34.3**
$HgOH^+$ ($^1A'$)	39.5	**38.4**; 104.1	1.984	1.335	1.84	43.4	**39.9**; 103.2
$HgSH^+$ ($^1A'$)	40.2	**51.5**; 53.0	2.353	1.017	0.80	41.2	**50.3**; 52.5
$HgSeH^+$ ($^1A'$)	41.1	53.7; **40.3**	2.487	0.911	0.89	40.8	51.5; **38.3**
$HgTeH^+$ ($^1A'$)	40.6	60.9; **28.2**	2.677	0.764	0.59	40.1	58.7; **23.0**
$HgOCF_3^+$ ($^1A'$)	33.8	**27.7**; 144.0	2.009	1.368	4.96	46.8	**32.7**; 157.1
HgO^+ ($^2\Pi^+$)	24.7	**24.0**; 187.4	1.997	1.314	2.22	22.2	**18.6**; 170.4
HgS^+ ($^2\Pi^+$)	33.9	**45.5**; 91.2	2.343	0.991	0.22	31.0	**40.2**; 85.4
$HgSe^+$ ($^2\Pi^+$)	36.3	**47.3**; 71.8	2.488	0.889	0.72	32.6	**41.6**; 62.3
$HgTe^+$ ($^2\Pi^+$)	37.5	57.3; **51.8**	2.668	0.774	0.49	32.6	51.8; **36.9**
HgF^+ ($^1\Sigma^+$)	54.3	38.2	1.943	1.539	3.73	57.6	38.3
$HgCl^+$ ($^1\Sigma^+$)	45.7	43.0	2.274	1.233	2.17	47.7	42.0
$HgBr^+$ ($^1\Sigma^+$)	43.8	41.2	2.428	1.109	2.56	44.5	39.5
HgI^+ ($^1\Sigma^+$)	39.9	49.2	2.598	0.949	2.21	39.2	47.2

traction of the 6s(Hg) orbital, the subsequent lowering of its orbital energy, and the stronger stabilization of the σ MO, which is valid for all X but the alkali atoms. The destabilization of the π* MOs increases with the number of π (lone pair) orbitals and with increasing electronegativity of X [adjustment of the *n*pπ orbital energy of X to the energy of the 5d(Hg) orbitals]. Hence, for F, Cl, Br, O, and OH, the lone pair effect dominates and makes the relativistic correction negative.

In the case of neutral HgX molecules, there the additional destabilizing effect of the σ* MO. A relativistically induced increase in the stabilization of the σ MO implies an even larger destabilization of the σ* MO so that the net effect becomes negative. Since the lone pair effect is also negative, the relativistic correction leads to a decrease in the BDE. From Cl to F (S to O; PH_2 to NH_2) a sudden drop of the relativistic correction by 5 to 6 kcal mol^{-1} (Table 5 a) can be observed. This drop again indicates the influence of the relativistically caused increase in π destabilization (lone pair repulsion) and confirms that HgX bonding can only be explained by considering both σ and π MOs.

2.3. Van der Waals Interactions

One could speculate that all weakly bonded HgX molecules are just van der Waals complexes rather than covalently bonded molecules. However, the magnitude of the BDE is not

Table 5. Non-relativistic BDE values and their relativistic corrections (in bold) for 28 HgX molecules.

HgX										
H	20.8									
	−10.8									
Li	4.1	CH_3	12.6	NH_2	18.7	OH	37.5	O	26.8	F	64.2
	−1.2		**−9.6**		**−14.5**		**−25.1**		**−23.3**		**−33.3**
Na	2.8	SiH_3	15.2	PH_2	12.7	SH	28.4	S	21.8	Cl	49.0
	−0.5		**−8.9**		**−9.1**		**−18.6**		**−16.1**		**−27.6**
K	0.6	GeH_3	14.2	AsH_2	10.6	SeH	23.9	Se	17.7	Br	41.1
	0.2		**−8.8**		**−6.1**		**−16.4**		**−14.0**		**−26.7**
Rb	0.2	SnH_3	10.1	SbH_2	6.0	TeH	18.0	Te	12.0	I	30.5
	0.5		**−7.1**		**−4.1**		**−12.1**		**−9.4**		**−19.6**
		CF_3	10.1			OCF_3	48.4				
			−7.4				**−26.2**				
		CN	55.5								
			−22.9								
HgX^+										
H	39.6									
	21.3									
Li	16.5	CH_3	45.8	NH_2	39.7	OH	43.4	O	22.2	F	57.6
	−2.7		**23.4**		**10.3**		**−3.5**		**−3.6**		**−19.3**
Na	15.7	SiH_3	51.7	PH_2	41.6	SH	41.2	S	31.0	Cl	47.7
	−9.5		**32.9**		**22.2**		**9.1**		**9.2**		**−5.7**
K	5.3	GeH_3	51.6	AsH_2	42.7	SeH	40.8	Se	32.6	Br	44.5
	−0.3		**32.9**		**24.0**		**10.7**		**9.0**		**−5.0**
Rb	4.2	SnH_3	50.6	SbH_2	42.6	TeH	40.1	Te	32.6	I	39.2
	0.2		**35.7**		**29.3**		**18.6**		**19.2**		**8.0**
		CF_3	25.0			OCF_3	46.8				
			22.3				**−14.1**				
		CN	49.4								
			3.8								

a reliable indicator for the nature of the bond. Instead we used the Cremer–Kraka criterion of covalent bonding, which is based on the properties of the electron density distribution $\rho(\mathbf{r})$ in the bond region.[56] A covalent bond is given when a path of maximum electron density with (3,−1) bond critical point $\mathbf{r}_c$ connects the interacting atoms (necessary condition) and the energy density at the bond critical point $H(\mathbf{r}_c)$ is negative (sufficient condition), which indicates a stabilizing effect of the bond density.[56]

Results of this analysis are summarized in Table 6. They reveal that HgX bonding is predominantly covalent although covalent bonding becomes weaker when moving X from right to the left of the periodic table and when increasing the atomic number of atom (or group) X. Thus, the weakest covalent bonds are found for HgX molecules with $X = SnH_3$ or SbH_2. This in line with the increase in the σ* destabilization energies [energy of the singly occupied orbital of SnH_3: −8.75 eV; Hg(6s) −8.8 eV, destabilization of σ*: 83.3 kcal mol^{-1}; Table 3]. Exceptions are found for the mercury alkali molecules (neutral and cations), which are all van der Waals molecules although their BDE values are not much different from those HgX molecules with $X = CH_3$, … , SnH_3 or NH_2, … SbH_2. The major difference, however, in the case of the alkali atoms results from their much higher electropositive character and the high-lying *n*s orbital of an alkali metal (Table 2) that act as a donor orbital. Two electronic effects lead to weak interactions only. A strong covalent bond cannot be formed because of the large energy difference between the 6s(Hg) and *ns*(alkali) orbitals ($\geq$3.5 eV, Table 2). At the same time, an ionic bond is also not possible since the 6p(Hg) orbitals are too high in energy to function as acceptor orbitals. Therefore just 0.02 to 0.03 electron (Table 1) are transferred from Hg to the alkali partner, which is too little to establish ionic bonding. Hence, all mercury–alkali molecules investigated herein are van der Waals complexes.[63]

The same holds for the corresponding mercury–alkali cations. The positive charge is predominantly localized at the alkali atom with less than 10% being delocalized to the Hg atom. The preferred dissociation follows reaction II, leading to BDE values between 3.3 (Rb) and 14.9 kcal mol^{-1} (Li, Table 4). Despite the relatively high BDE for HgLi, the corresponding bond is also noncovalent and typical of a van der Waals bond.

We reoptimized the bond lengths of all van der Waals complexes HgX at the NESC/CCSD(T) level to verify the type of bonding. Interaction distances became slightly longer (Table 1), however BDEs changed only by $\leq$0.1 kcal mol^{-1}. In all cases, van der Waals interactions and the absence of covalent interaction were confirmed.

3. Comparison with Experimental Bond Dissociation Enthalpies BDH

For a comparison of calculated BDEs with experimental results, the former have to be converted to BDH (bond dissociation enthalpies at 298 K) values by determining zero-point energies and thermal corrections. In addition, one has to consider SOC. Significant changes in the BDE values due to SOC will only occur if bonding leads to a fractional occupation of the p- and d-orbitals of Hg. This was however not observed for the HgX molecules investigated (see discussion of calculated NBO values above) and therefore SOC effects were not considered herein. Peterson and co-workers thoroughly investigated the energetic consequences of SOC in the case of the mercury chalcogenides using MRCI theory and found that the BDE changed by less than 2 kcal mol^{-1}.[59] However for HgO, SOC-induced avoided crossing leads to a singlet rather than a triplet ground state as found herein.

Table 7 reveals that NESC/CCSD(T) values and experimental BDHs agree reasonably where one has to consider experimental error bars and the 1–2 kcal mol^{-1} changes resulting from

Table 6. Description of HgX bonding.

Molecule	Electron Density ρ(rc) [electron/Å3]	Energy Density H(rc) [hartree/Å3]	Bond Character	Cation	Electron Density ρ(rc) [electron/Å3]	Energy Density H(rc) [hartree/Å3]	Bond Character
A) HgX				B) HgX^+			
HgH ($^2\Sigma^+$)	0.681	−0.331	covalent	HgH^+ ($^1\Sigma^+$)	1.004	−0.751	covalent
HgLi ($^2\Sigma^+$)	0.069	0.004	vdW	$HgLi^+$ ($^1\Sigma^+$)	0.099	0.006	vdW
HgNa ($^2\Sigma^+$)	0.053	0.002	vdW	$HgNa^+$ ($^1\Sigma^+$)	0.074	0.011	vdW
HgK ($^2\Sigma^+$)	0.037	0.002	vdW	HgK^+ ($^1\Sigma^+$)	0.053	0.006	vdW
HgRb ($^2\Sigma^+$)	0.032	0.001	vdW	$HgRb^+$ ($^1\Sigma^+$)	0.048	0.004	vdW
$HgCH_3$ ($^2A_1$)	0.338	−0.079	weak covalent	$HgCH_3^+$ ($^1A_1$)	0.641	−0.239	covalent
$HgSiH_3$ ($^2A_1$)	0.346	−0.094	weak covalent	$HgSiH_3^+$ ($^1A_1$)	0.349	−0.157	covalent
$HgGeH_3$ ($^2A_1$)	0.297	−0.044	weak covalent	$HgGeH_3^+$($^1A_1$)	0.341	−0.029	weak covalent
$HgSnH_3$ ($^2A_1$)	0.233	−0.038	weak covalent	$HgSnH_3^+$($^1A_1$)	0.262	−0.046	weak covalent
HgCN ($^2\Sigma^+$)	0.688	−0.241	covalent	$HgCN^+$ ($^1\Sigma^+$)	0.945	−0.485	covalent
$HgCF_3$ ($^2A_1$)	0.229	−0.025	weak covalent	$HgCF_3^+$ ($^1A_1$)	0.505	−0.140	covalent
$HgNH_2$ ($^2A'$)	0.409	−0.075	weak covalent	$HgNH_2^+$ ($^1A'$)	0.808	−0.328	covalent
$HgPH_2$ ($^2A'$)	0.266	−0.040	weak covalent	$HgPH_2^+$ ($^1A'$)	0.478	−0.160	covalent
$HgAsH_2$ ($^2A'$)	0.208	−0.022	weak covalent	$HgAsH_2^+$($^1A'$)	0.402	−0.076	weak covalent
$HgSbH_2$ ($^2A'$)	0.174	−0.018	weak covalent	$HgSbH_2^+$($^1A'$)	0.297	−0.060	weak covalent
HgOH ($^2A'$)	0.571	−0.146	covalent	$HgOH^+$ ($^1A'$)	0.914	−0.405	covalent
HgSH ($^2A'$)	0.401	−0.079	weak covalent	$HgSH^+$ ($^1A'$)	0.618	−0.214	covalent
HgSeH ($^2A'$)	0.309	−0.043	weak covalent	$HgSeH^+$ ($^1A'$)	0.509	−0.134	covalent
HgTeH ($^2A'$)	0.272	−0.041	weak covalent	$HgTeH^+$ ($^1A'$)	0.407	−0.105	covalent
$HgOCF_3$ ($^2A'$)	0.860	−0.356	covalent	$HgOCF_3^+$($^1A'$)	0.558	−0.136	covalent
HgO ($^3\Pi$)	0.512	−0.107	covalent	HgO^+ ($^2\Pi$)	0.932	−0.418	covalent
HgS ($^3\Pi$)	0.391	−0.073	weak covalent	HgS^+ ($^2\Pi$)	0.629	−0.220	covalent
HgSe ($^3\Pi$)	0.275	−0.031	weak covalent	$HgSe^+$ ($^2\Pi$)	0.509	−0.132	covalent
HgTe ($^3\Pi$)	0.260	−0.036	weak covalent	$HgTe^+$ ($^2\Pi$)	0.414	−-0.108	covalent
HgF ($^2\Sigma^+$)	0.652	−0.163	polar covalent	HgF^+ ($^1\Sigma^+$)	0.948	−0.401	polar covalent
HgCl ($^2\Sigma^+$)	0.484	−0.107	polar covalent	$HgCl^+$ ($^1\Sigma^+$)	0.709	−0.250	polar covalent
HgBr ($^2\Sigma^+$)	0.365	−0.056	weak covalent	$HgBr^+$ ($^1\Sigma^+$)	0.576	−0.167	covalent
HgI ($^2\Sigma^+$)	0.325	−0.042	weak covalent	HgI^+ ($^1\Sigma^+$)	0.484	−0.142	covalent

SOC corrections. However, in the case of the mercury chalcogenides (X = O, S, Se, Te) experimental and calculated bond dissociation energies differ by 30–50 kcal mol^{-1}. Shepler and Peterson[18] and Tossell[29,30] have made the same observation in the case of HgO without attempting to explain the discrepancy between theory and experiment. Filatov and Cremer[19] investigated HgO, HgS, and HgSe at the ZORA-GI and IORAmm levels of theory and showed that observations made for HgO seem to apply to all mercury chalcogenides. This is confirmed by the data given in Table 7 and Table 3 and by the recent study of Peterson and co-workers.[59]

Table 7. Comparison of experimental and calculated bond dissociation enthalpies BDH(298).[a]

Molecule (State)	NESC/CCSD(T) [kcal mol^{-1}]	exp [kcal mol^{-1}]	Molecule (State)	NESC/CCSD(T) [kcal mol^{-1}]	exp [kcal mol^{-1}]
HgH ($^2\Sigma^+$)	9.2	9.5	$HgCH_3$ ($^2A_1$)	1.5	1.4–5.3
HgLi ($^2\Sigma^+$)	3.2	3.3	HgO ($^3\Pi$)	3.8	52.8
HgNa ($^2\Sigma^+$)	2.6	2.2	HgS ($^3\Pi$)	6.0	51.9
HgK ($^2\Sigma^+$)	1.1	2.0	HgSe ($^3\Pi$)	4.0	34.5
HgRb ($^2\Sigma^+$)	1.0	2.0	HgTe ($^3\Pi$)	2.9	<34
HgF ($^2\Sigma^+$)	31.0	32.8	HgO ($^1\Sigma^+$)	48.5	52.8
HgCl ($^2\Sigma^+$)	21.6	24; 25.1	HgS ($^1\Sigma^+$)	33.0	51.9
HgBr ($^2\Sigma^+$)	14.7	16.6; 16.4	HgSe ($^1\Sigma^+$)	29.5	34.5
HgI ($^2\Sigma^+$)	11.2	8.4	HgTe ($^1\Sigma^+$)	31.3	<34

[a] Eperimental BDH values from refs. [20, 62]. For HgE($^1\Sigma^+$) dissociation into Hg(^{1}S) + E(^{1}D) is given, although this does not comply with the results of SOC. BDH values have been calculated using NESC/CCSD(T) values for the BDE of HgO ($^1\Sigma^+$)→Hg(^{1}S) + E(^{3}P) and adding the experimental excitation energy E(^{3}P)→E(^{1}D) from ref. [60].

When adjusting the MO diagram to the valence electron configuration of a chalcogene E (6 rather than 7 electrons when compared to halogen, Figure 2), a singlet ground state ($^1\Sigma^+$) is predicted for HgE and this is confirmed for HgS and HgSe when using large basis sets.[59,64] In the case of HgO and HgTe, the $^3\Pi$ state is somewhat more stable (1.3 kcal mol^{-1}) and becomes (without SOC) the ground state as discussed by Filatov and Cremer[19] (see also refs. [18, 59]). Although the σ^* MO is no longer

occupied in the $^1\Sigma^+$ state, thus leading to a full σ bond, bonding is still weakened by the destabilizing interactions of four π* electrons (lone pair repulsion). In the $^3\Pi$ state, lone-pair repulsion is reduced for the price that the σ* MO is occupied, which leads to a destabilization energy of about 15 kcal mol^{-1} in the case of HgO. Obviously, the reduction in lone pair repulsion outweighs the destabilization of the σ* MO by a few kcal mol^{-1}. We note in this connection that the two states differ considerably with regard to charge transfer ($^3\Pi$: 0.428 electron; $^1\Sigma^+$: 0.903 electron), dipole moment (2.05 vs 5.55 Debye), and HgO bond length (2.231 vs 1.875 Å). Clearly, the $^3\Pi$ state benefits from a longer bond length in the way that lone pair repulsion is further reduced. On the other hand, there is also a reduction in charge transfer and ionic character of the bond, which lead to a weakening of the bond.

3.1. Dissociation of Mercury Chalcogenides

In the $^3\Pi$ ground state, a mercury chalcogenide HgE (E = O, Te) will dissociate to Hg(^{1}S) + E(^{3}P). Since this dissociation requires less than 6 kcal mol^{-1}, these mercury chalcogenides HgE($^3\Pi$) should rapidly decompose in the gas phase under normal conditions. Their detection may only be possible under matrix isolation conditions at low temperatures. Molecules HgE in their $^1\Sigma^+$ state should decompose to Hg(^{1}S) + E(^{1}D), which would imply BDE values of 48.3 (E = O), 32.7 (S), 29.2 (Se), and 31.0 kcal mol^{-1} (Te) in much better agreement with experiment (see Table 7).

However, this prediction does not consider SOC, which has important consequences for the dissociation of HgE($^1\Sigma^+$). Shepler and Peterson showed on the basis of MRCI calculations[18] that for HgO there is a SOC-induced avoided crossing between the $\Omega = 0^+$ components of the $^1\Sigma^+$ and $^3\Pi$ state that leads to a dissociation of the $^1\Sigma_0{}^+$ state to the $^3P_2$ ground state of oxygen rather than its ^{1}D excited state. Hence, the dilemma that there is still a large difference between calculated and experimental BDE values remains in this case. Theory suggests that the HgO monomers cannot be detected experimentally at room temperature.

In the case of HgS, Cressiot and co-workers[64] found on the basis of large-scale MRCI calculations that, after including SOC, the $X^1\Sigma_0{}^+$ state is 3.5 kcal mol^{-1} below the $A^3\Pi_2$ state. These authors estimated an effective dissociation energy of 6.5 cal mol^{-1} for HgS($X^1\Sigma_0{}^+$), which again should make the experimental observation of this molecule rather difficult. Similarly difficult should be the experimental detection of HgSe and HgTe (SOC-corrected dissociation energies of 4.8 and 2.8 kcal mol^{-1}, respectively, in their ground states).[59]

Filatov and Cremer[19] have suggested that the mass-spectrometric investigation of HgE molecules[65] were flawed by the fact that mixtures of HgE dimers and trimers were measured. Such an error is unlikely under normal conditions, because the natural distribution of Hg and E isotopes should lead to m/e signals clearly different for monomer, dimer, and trimer. However, in the case of the mercury chalcogenides, the m/e signals of the target molecules could not be observed directly and measurements were therefore based on a number of assumptions. Presently, we are investigating HgE dimers and trimers, and their ionization and fragmentation patterns to shed further light on the extraordinary discrepancy between theory and experiment in the case of the mercury chalcogenides.

4. Chemical Relevance

Bonding in neutral and charged HgX compounds reaches from fractions of a kcal mol^{-1} up to 60 kcal mol^{-1} (Tables 1 and 4, Table 3) where however the majority of the neutral molecules considered possess BDE values between 1 and 12 kcal mol^{-1}. Of these molecules, only the mercury alkali molecules and their cations are genuine van der Waals complexes. The preferred bonding mode in all other HgX molecules and cations is covalent—best described by a three-electron two-orbital model. Covalent HgX bonding is weakened by the destabilization of the σ* MO and lone-pair repulsion. It is strengthened by ionic contributions to bonding in dependence of the electronegativity of the partner atom (group). Destabilization of the σ* MO, lone pair repulsion, and ionic contribution to bonding are fine-tuned by scalar relativistic corrections leading to 6s(Hg) orbital contraction and 5d(Hg) orbital expansion. Also, the suppression of 6p orbital participation in bonding is a consequence of relativistic effects as 6s orbital contraction increases the energy gap between 6s and 6p orbitals for Hg.

The magnitude of σ destabilization can be assessed with the thermodynamic cycle of Scheme 1, from the energy difference BDE(HgX) − BDE(HgX^+) that is largest for group Vb and IVb bonding partners and decreases with increasing electronegativity and ionic character of bonding. The σ destabilization energy is recovered upon ionization of HgX, which is the reason why Hg–alkali cations have much stronger bonds than their neutral counterparts (Table 3). In this connection, it has to be emphasized that the charge distribution in HgX (HgX^+) reflects the effective electronegativity of the partner atom or group of Hg, which is often not identical to that of free X in its equilibrium state. Dissociation of HgX^+ often proceeds in a different way than the charge distribution may suggest, as is obvious from the data in Table 4.

Lone-pair repulsion involving the mercury 5d AOs plays an important role for the stability of HgX and HgX^+ molecules. It is decisive in the case of the mercury chalcogenides where it can be larger than σ destabilization, thus leading in some cases (E = O, Te) to $^3\Pi$ rather than $^1\Sigma^+$ ground states. When E = O, avoided crossing induced by SOC leads to low dissociation energies for both HgE($^3\Pi$) and HgE($^1\Sigma^+$), none of which should be experimentally detectable under normal conditions.

These findings have important consequences for 1) mercury bonding in HgX_2 and other compounds, 2) the chemistry of elemental Hg in the atmosphere. Once a HgX monomer is formed, charge transfer from Hg to X (X being electronegative) leads to a partially positively charged Hg atom that is prone to form a second very stable bond with another atom X since the situation resembles that of bond formation in HgX^+ (Table 3). This is revealed in Table 8 where some HgX_2 BDEs, and BDHs are summarized together with the corresponding bond length and charge transfer data. In the case of $Hg(CH_3)_2$, the BDE for

Table 8. NESC/B3LYP Properties of HgX_2 molecules.[a]

Molecule	HgX Bond Length [Å]	Charge q(Hg) [electron]	AE [kcal mol^{-1}]	AH(298) [kcal mol^{-1}]	BDE [kcal mol^{-1}]	BDH(298) [kcal mol^{-1}]
HgH_2	1.650 (1.647)	0.814	88.6	82.9 (79.8)	76.8	72.1 (70.0)
$Hg(CH_3)_2$[b]	2.118 (2.09)	1.012	60.3	55.8 (59.0)	58.6	55.1 (55.2)
HgF_2	1.933	1.401	123.2	122.4 (122.6)	89.6	88.7 (89.8)
$HgCl_2$	2.288 (2.28)	1.131	98.6	98.1 (107.8)	75.9	75.3 (82.7)
$HgBr_2$	2.463 (2.40)	1.023	78.6	78.4 (88.6)	62.5	62.1 (72.0)
HgI_2	2.617 (2.57)	0.882	73.2	73.1 (69.7)	59.6	59.2 (61.3)

[a] Atomization energies AE for the reaction: $HgX_2 \rightarrow Hg + 2X$, corresponding atomization enthalpies AH(298); bond dissociation energies BDE for the dissociation: $HgX_2 \rightarrow HgX + X$, corresponding bond dissociation enthalpies BDH(298); experimental values in parentheses.[20,61] [b] R(CH) = 1.089 Å, $<$HgCH = 110.2°.

dissociation into $HgX + X$ is 58.6 kcal mol^{-1} (BDE of HgX^+ is 69 kcal mol^{-1}, Table 3) whereas the total atomization energy is 60.3 kcal mol^{-1} (BDE of HgX is 3 kcal mol^{-1}), thus suggesting bond strengths of 30.2 kcal mol^{-1} for each HgX bonds.

Similarly, we calculate rather high dimerization and trimerization energies, where the corresponding reactions are driven by the partial positive (negative) charge at Hg (X) and the electrostatic attraction of the monomer units. This continues to be a driving force until HgX units are combined via oligomeric and polymeric intermediates to solid material.

It has been asked in the introduction whether the elemental mercury of the atmosphere can be oxidized by BrO to HgO, which then may react with water to yield Hg^{II}. Hg^{II} is then deposited, in form of various compounds, on the earth surface and in the ocean. However this reaction sequence can be excluded on the basis of theoretical calculations carried out herein and in the studies of others.[18–30] The reaction of elemental Hg with OH radicals is more likely considering a reaction energy of 12 kcal mol^{-1}. Similarly, the reaction with Cl or Br atoms should play a role in the atmosphere.

Acknowledgement

E.K. and D.C. thank the National Science foundation and the University of the Pacific for financial support. Discussions with F. Axe, who also did some NESC calculations, are acknowledged.

Keywords: bond energy · bond theory · electronic structure · mercury · relativistic quantum chemistry

[1] L. Friberg, J. Vostal, *Mercury in the Environment*, CRC, Cleveland, **1972**, pp. 1–186.
[2] P. J. Craig, *Organometallic compounds in the Environment*, Longman, London, **1986**.
[3] J. E. Fergusson, *The Heavy Elements: Chemistry, Environmental Impact and Health Effects*, Pergamon, Oxford, **1990**.
[4] M. Morita, J. Yoshinaga, J. S. Edmonds, *Pure Appl. Chem.* **1998**, *70*, 1585.
[5] W. F. Fitzgerald in *Chemical Oceanography* (Eds.: J. P. Riley, R. Chester, R. A. Duce), Academic Press, New York, **1989**.
[6] T. A. Jackson, *Environ. Rev.* **1997**, *5*, 99.
[7] M. H. Keating, *Mercury Study Report to Congress, Vol. 1: Executive Summary.* United States Environmental Protection Agency, **1997**.
[8] L. Friberg, G. F. Nordberg, V. B. Vouk, *Handbook on the Toxicology of Metals, Vol. 11*, Elsevier, Amsterdam, **1986**.
[9] R. Ebinghaus, H. H. Kock, C. Temme, J. W. Einax, A. G. Lowe, A. Richter, J. P. Burrows, W. H. Schroeder, *Environ. Sci. Technol.* **2002**, *36*, 1238.
[10] J. Y. Lu, W. H. Schroeder, L. A. Barrie, A. Steffen, H. E. Welch, K. Martin, L. Lockhart, R. V. Hunt, G. Boila, A. Richter, *Geophys. Res. Lett.* **2001**, *28*, 3219.
[11] W. H. Schroeder, K. G. Anlauf, L. A. Barrie, J. Y. Lu, A. Steffen, D. R. Schneeberger, T. Berg, *Nature* **1998**, *394*, 331.
[12] A. Steffen, W. H. Schroeder, J. W. Bottenheim, J. Narayan, J. D. Fuentes, *Atmos. Environ.* **2002**, *36*, 2653.
[13] S. E. Lindberg, S. Brooks, C.-J. Lin, K. J. Scott, M. S. Landis, R. K. Stevens, M. Goodsite, A. Richter, *Environ. Sci. Technol.* **2002**, *36*, 1245.
[14] T. Berg, J. Bartnicki, J. Munthe, H. Lattila, J. Hrehoruk, A. Mazur, *Atmos. Environ.* **2001**, *35*, 2569.
[15] L. A. Barrie, J. W. Bottenheim, R. C. Schnell, P. J. Crutzen, R. A. Rasmussen, *Nature* **1988**, *334*, 138.
[16] H. Boudries, J. W. Bottenheim, *Geophys. Res. Lett.* **2000**, *27*, 517.
[17] K. L. Foster, R. A. Plastridge, J. W. Bottenheim, P. B. Shepson, B. J. Finlayson-Pittsand, C. W. Spicer, *Science* **2001**, *291*, 471.
[18] B. C. Shepler, K. A. Peterson, *J. Phys. Chem. A* **2003**, *107*, 1783.
[19] M. Filatov, D. Cremer, *ChemPhysChem* **2004**, *5*, 1547.
[20] K. P. Huber, G. Herzberg, *Molecular Spectra and Molecular Structure IV. Constants of Diatomic Molecules*, Van Nostrand Reinhold, New York, **1979**.
[21] B. C. Shepler, N. B. Balabanov, K. A. Peterson, *J. Chem. Phys.* **2007**, *127*, 164304.
[22] B. C. Shepler, A. D. Wright, N. B. Balabanov, K. A. Peterson, *J. Phys. Chem. A* **2007**, *111*, 11342.
[23] K. A. Peterson, B. C. Shepler, J. M. Singleton, *Mol. Phys.* **2007**, *105*, 1139.
[24] B. C. Shepler, N. B. Balabanov, K. A. Peterson, *J. Phys. Chem. A* **2005**, *109*, 10363.
[25] N. B. Balabanov, B. C. Shepler, K. A. Peterson, *J. Phys. Chem. A* **2005**, *109*, 8765.
[26] N. B. Balabanov, K. A. Peterson, *J. Chem. Phys.* **2004**, *120*, 6585.
[27] N. B. Balabanov, K. A. Peterson, *J. Chem. Phys.* **2003**, *119*, 12271.
[28] N. B. Balabanov, K. A. Peterson, *J. Phys. Chem. A* **2003**, *107*, 7465.
[29] J. A. Tossell, *J. Phys. Chem. A* **2006**, *110*, 2571.
[30] J. A. Tossell, *J. Phys. Chem. A* **2003**, *107*, 7804.
[31] J. A. Tossell, *J. Phys. Chem. A* **2001**, *105*, 935.
[32] J. A. Tossell, *Am. Mineral.* **1999**, *84*, 877.
[33] J. A. Tossell, *J. Phys. Chem. A* **1998**, *102*, 3587.
[34] M. E. Goodsite, J. M. Plane, H. Skov, *Environ. Sci. Technol.* **2004**, *38*, 1772.
[35] A. F. Khalizov, B. Viswanathan, P. Larregaray, P. A. Ariya, *J. Phys. Chem. A* **2003**, *107*, 6360.
[36] A. Hu, P. Otto, J. Ladik, *J. Mol. Struct. Theochem* **1999**, *468*, 163.
[37] a) T. R. Cundari, E. W. Moody, *J. Mol. Struct. Theochem* **1998**, *425*, 43; b) M. Kaupp, H. G. von Schnering, *Inorg. Chem.* **1994**, *33*, 2555.
[38] M. Liao, Q. Zhang, W. H. E. Schwarz, *Inorg. Chem.* **1995**, *34*, 5597.
[39] V. Barone, A. Bencini, T. Federico, M. G. Uytterhoeven, *J. Phys. Chem.* **1995**, *99*, 12743.
[40] S. T. Howard, *J. Phys. Chem.* **1994**, *98*, 6110.

[41] M. Kaupp, M. Dolg, H. Stoff, H. J. v. Schnering, *Inorg. Chem.* **1994**, *33*, 2122.
[42] P. P. D. Schwerdtfeger, W. Boyd, S. Brieen, J. S. McFeaters, M. Dolg, M. S. Liao, E. W. H. Schwarz, *Inorg. Chim. Acta* **1993**, *213*, 233.
[43] D. Strömberg, A. Strömberg, U. Wahlgren, *Water Air Soil Pollut.* **1991**, *56*, 681.
[44] D. Strömberg, O. Gropen, U. Wahlgren, *Chem. Phys.* **1989**, *133*, 207.
[45] M. Filatov, D. Cremer, *J. Chem. Phys.* **2005**, *122*, 044104.
[46] A. D. Becke, *J. Chem. Phys.* **1993**, *98*, 5648.
[47] A. D. Becke, *Phys. Rev. A* **1988**, *38*, 3098.
[48] C. Lee, W. Yang, R. G. Parr, *Phys. Rev. B* **1988**, *37*, 785.
[49] M. Filatov, K. G. Dyall, *Theor. Chem. Acc.* **2007**, *117*, 333.
[50] K. Raghavachari, G. W. Trucks, J. A. Pople, M. Head-Gordon, *Chem. Phys. Lett.* **1989**, *157*, 479.
[51] a) Hg: K. G. Dyall, *Theor. Chem. Acc.* **2004**, *112*, 403; b) 4p elements: K. G. Dyall, *Theor. Chem. Acc.* **1998**, *99*, 366; addendum K. G. Dyall, *Theor. Chem. Acc.* **2002**, *108*, 365; revision K. G. Dyall, *Theor. Chem. Acc.* **2006**, *115*, 441; available from http://dirac.chem.sdu.dk; c) Rb: available from http://dirac.chem.sdu.dk.
[52] S. F. Boys, F. Bernardi, *Mol. Phys.* **1970**, *19*, 553.
[53] cc-pVTZ Dunning basis sets: a) T. H. Dunning, Jr., *J. Chem. Phys.* **1989**, *90*, 1007; b) D. E. Woon, T. H. Dunning, Jr., *J. Chem. Phys.* **1993**, *98*, 1358; c) D. E. Woon, T. H. Dunning, Jr., *J. Chem. Phys.* **1994**, *100*, 2975; d) A. K. Wilson, D. E. Woon, K. A. Peterson, T. H. Dunning, Jr., *J. Chem. Phys.* **1999**, *110*, 7667.
[54] J. P. Blaudeau, M. P. McGrath. L. A. Curtiss, *J. Chem. Phys.* **1997**, *107*, 5016.
[55] A. E. Reed, L. A. Curtiss, E. Weinhold, *Chem. Rev.* **1988**, *88*, 899.
[56] a) D. Cremer, E. Kraka, *Angew. Chem.* **1984**, *96*, 612; *Angew. Chem. Int. Ed. Engl.* **1984**, *23*, 627; b) D. Cremer, E. Kraka, *Croat. Chem. Acta* **1984**, *57*, 1259.
[57] E. Kraka, J. Gräfenstein, M. Filatov, H. Joo, D. Izotov, J. Gauss, Y. He, A. Wu, V. Polo, L. Olsson, Z. Konkoli, Z. He, D. Cremer, COLOGNE08. Stockton, CA, University of Pacific, **2008**.
[58] M. J. Frisch, G. W. Trucks, H. B. Schlegel, G. E. Scuseria, M. A. Robb, J. R. Cheeseman, J. A. Montgomery, Jr., T. Vreven, K. N. Kudin, J. C. Burant, J. M. Millam, S. S. Iyengar, J. Tomasi, V. Barone, B. Mennucci, M. Cossi, G. Scalmani, N. Rega, G. A. Petersson, H. Nakatsuji, M. Hada, M. Ehara, K. Toyota, R. Fukuda, J. Hasegawa, M. Ishida, T. Nakajima, Y. Honda, O. Kitao, H. Nakai, M. Klene, X. Li, J. E. Knox, H. P. Hratchian, J. B. Cross, V. Bakken, C. Adamo, J. Jaramillo, R. Gomperts, R. E. Stratmann, O. Yazyev, A. J. Austin, R. Cammi, C. Pomelli, J. W. Ochterski, P. Y. Ayala, K. Morokuma, G. A. Voth, P. Salvador, J. J. Dannenberg, V. G. Zakrzewski, S. Dapprich, A. D. Daniels, M. C. Strain, O. Farkas, D. K. Malick, A. D. Rabuck, K. Raghavachari, J. B. Foresman, J. V. Ortiz, Q. Cui, A. G. Baboul, S. Clifford, J. Cioslowski, B. B. Stefanov, G. Liu, A. Liashenko, P. Piskorz, I. Komaromi, R. L. Martin, D. J. Fox, T. Keith, M. A. Al-Laham, C. Y. Peng, A. Nanayakkara, M. Challacombe, P. M. W. Gill, B. Johnson, W. Chen, M. W. Wong, C. Gonzalez, J. A. Pople, *Gaussian 03 (Revision C.02)*, Gaussian, Inc., Wallingford, CT, **2004**.
[59] K. A. Peterson, B. C. Shepler, J. M. Singleton, *Mol. Phys.* **2007**, *105*, 1139.
[60] C. E. Moore, *Atomic Energy Levels*, NSRDS-NBS 35 U. S. GPO, Washington, D. C., **1971**.
[61] P.-A. Glans, T. Learmonth, C. McGuinness, K. E. Smith, J. Guo, A. Walsh, G. W. Watson, R. G. Egdell, *Chem. Phys. Lett.* **2004**, *399*, 98.
[62] a) *Handbook of Chemistry and Physics, 72nd ed.* (Ed.: D. R. Lide), CRC, Boca Raton, **1992**; b) NIST Chemistry WebBook, NIST Standard Reference Database Number 69, June 2005 Release, http://webbook.nist.gov/chemistry/; c) HgH_2: A. Shayesteh, S. Yu, P. F. Bernath, *Chem. Eur. J.* **2005**, *11*, 4709–4712.
[63] L. Thiel, H. Hotop, W. Meyer, *J. Chem. Phys.* **2003**, *119*, 9008, and references therein.
[64] C. Cressiot, M. Guitou, A. Mitrushchenkov, G. Chambaud, *Mol. Phys.* **2007**, *105*, 1207.
[65] M. Grade, W. Hirschwald, *Ber. Bunsen-Ges.* **1982**, *86*, 899.

Received: August 6, 2008
Published online on November 14, 2008

